Synthesis and Design of Novel Tetranuclear and Dinuclear Gold(I) Phosphine Acetylide Complexes. First X-ray Crystal Structures of a Tetranuclear ([Au_4(tppb)(C≡CPh)$_4$]) and a Related Dinuclear ([Au_2(dppb)(C≡CPh)$_2$]) Complex

Vivian Wing-Wah Yam,* Sam Wing-Kin Choi, and Kung-Kai Cheung

Department of Chemistry, The University of Hong Kong, Pokfulam Road, Hong Kong

Received July 28, 1995[⊗]

Reaction of [Au(C≡CR)]$_\infty$ with dppb and tppb in CH_2Cl_2 afforded the corresponding luminescent Au_2(dppb)(C≡CR)$_2$ and Au_4(tppb)(C≡CR)$_4$ (dppb = 1,4-bis(diphenylphosphino)-benzene; tppb = 1,2,4,5-tetrakis(diphenylphosphino)benzene; R = C_6H_{13}, Ph, 4-MeO-Ph); their photophysical properties have been studied, and the X-ray crystal structures of Au_2(dppb)(C≡CPh)$_2$ (**2**) and Au_4(tppb)(C≡CPh)$_4$ (**5**) have been determined. Close Au···Au contacts are present in **5**, which twisted the six-membered ring that comprises the PAu_2PC_2 unit. Such a structure is reminiscent of a distorted anthracene-like unit containing Au atoms as part of the heterocycle, owing to the auriophilicity which brings the Au atoms into close contact.

Introduction

Recently, the study and design of novel materials with unique physical properties have become the focus of much interest.[1] In our recent efforts on the synthesis, characterization, and luminescent properties of acetylide-bridged metal complexes,[2] a series of related polynuclear Au(I) acetylides have been explored. In view of the preference of metal complexes with d^{10} electronic configuration to form linear two-coordinate species, they may serve as good and attractive candidates for the design of rigid-rod materials which may find applications in areas of materials science such as liquid crystal technology.[3] However, to our surprise, the design of liquid crystalline materials with d^{10} Au(I) is relatively rare.[4] In this paper, we report on the synthesis and characterization of binuclear Au_2(dppb)(C≡CC_6H_{13})$_2$ (**1**) and tetranuclear Au_4(tppb)(C≡CC_6H_{13})$_4$ (**4**) with short Au···Au contacts (dppb = 1,4-bis(diphenylphosphino)-benzene; tppb = 1,2,4,5-tetrakis(diphenylphosphino)-benzene). In **1**, the oct-1-ynyl groups serve as the flexible peripheral chains. This, together with the rigid central phosphine backbone, is expected to give one-dimensional compounds with potential calamitic mesogenic properties. On the other hand, when the bridging phosphine is changed from dppb to tppb, compound **4** is constructed with the acetylide groups extended in a two-dimensional array. These organometallic Au(I) phosphine acetylides have been shown to exhibit rich photophysics with long-lived emission. Their photophysics and spectroscopy together with those of other related complexes Au_2(dppb)(C≡CR)$_2$ (R = Ph (**2**), 4-MeO-Ph (**3**)) and Au_4(tppb)(C≡CR)$_4$ (R = Ph (**5**), 4-MeO-Ph) (**6**)) will also be described. The X-ray crystal structures of **2** and **5** have been determined.

Experimental Section

Materials and Reagents. Potassium tetrachloroaurate(III), phenylacetylene, and oct-1-yne were obtained from Aldrich Chemical Co. (4-Methoxyphenyl)acetylene was obtained from Maybridge Chemical Co. Ltd. [Au(C≡CR)]$_\infty$,[5a] dppb,[5b] and tppb[5b] were prepared by published methods. All solvents were purified and distilled by standard procedures before use. All other reagents were of analytical grade and were used as received.

Preparation of Complexes. All reactions were carried out under a stream of dry nitrogen at room temperature.

[Au_2(dppb)(C≡CC_6H_{13})$_2$] (1). To a dichloromethane solution of [Au(C≡CC_6H_{13})]$_\infty$ (100 mg, 0.327 mmol) was added a solid sample of dppb (73 mg, 0.164 mmol). After it was stirred for 15 min, the solution was concentrated and white solid was precipitated by addition of *n*-hexane. Recrystallization was accomplished by the slow diffusion of *n*-hexane vapor into a dichloromethane solution of the solid to give colorless crystals (yield 130 mg, 75%). ^{1}H NMR (270 MHz, CD_2Cl_2, 298 K, relative to TMS): δ 0.88 (t, 6H, $-CH_3$), 1.12−1.51 (m, 16H, $-CH_2-$), 2.24 (t, 4H, $-C\equiv CCH_2-$), 7.45−7.60 (m, 24H, dppb). Positive FAB-MS: *m*/*z* 1058 $(M)^+$, 951 $(M - \text{octynyl})^+$. IR (Nujol): ν/cm^{-1} 2133 (vw, C≡C). Anal. Calcd for $C_{46}H_{50}Au_2P_2\cdot 0.5CH_2Cl_2$: C, 50.71; H, 4.63. Found: C, 50.93; H, 4.41.

[Au_2(dppb)(C≡CPh)$_2$] (2). To a yellow suspension of [Au(C≡CPh)]$_\infty$ (100 mg, 0.336 mmol) in CH_2Cl_2 was added a solid sample of dppb (75 mg, 0.168 mmol). A clear yellow solution was obtained, and the mixture was stirred for 15 min. The solution was then concentrated, and *n*-hexane was added to precipitate the yellow products. Recrystallization was accomplished by the slow diffusion of diethyl ether vapor into a dichloromethane solution of the solid to give yellow crystals

⊗ Abstract published in *Advance ACS Abstracts,* February 1, 1996.

(1) (a) Bruce, D. W.; O'Hare, D. *Inorganic Materials*; Wiley: New York, 1992. (b) Bruce D. W.; Holbrey, J. D.; Tajbakhsh, A. R.; Tiddy, G. J. T. *J. Mater. Chem.* **1993**, *3*, 905. (c) Bruce, D. W. *Adv. Mater.* **1994**, *6*, 699.

(2) (a) Yam, V. W.-W.; Lee, W. K.; Lai, T. F. *Organometallics* **1993**, *12*, 2383. (b) Yam, V. W.-W.; Chan, L. P.; Lai, T. F. *Organometallics* **1993**, *12*, 2197. (c) Müller, T. E.; Choi, S. W. K.; Mingos, D. M. P.; Murphy, D.; Williams, D. J.; Yam, V. W.-W. *J. Organomet. Chem.* **1994**, *484*, 209.

(3) Collings, P. J. *Liquid Crystals*; Princeton University Press: Princeton, NJ, 1990.

(4) Kaharu, T.; Ishii, R.; Adachi, T.; Yoshida, T.; Takahashi, S. *J. Mater. Chem.* **1995**, *5*, 687.

(5) (a) Coates, G. E.; Parkin, C. *J. Chem. Soc.* **1962**, 3220. (b) Christina, H.; McFarlane, E.; McFarlane, W. *Polyhedron* **1988**, *7*, 1875.

0276-7333/96/2315-1734$12.00/0

(yield 122 mg, 70%). ^{1}H NMR (270 MHz, CD_2Cl_2, 298 K, relative to TMS): δ 7.06−7.57 (m, 10H, −C≡CPh; 24H, dppb). Positive FAB-MS: *m/z* 941 $(M - C{\equiv}CPh)^+$. IR (Nujol): ν/cm^{-1} 2125 (vw, C≡C).

[Au_2(dppb)(C≡C(4-MeO-Ph))$_2$] (3). The procedures were similar to those for **2**, except $[Au(C{\equiv}C(4\text{-MeO-Ph})]_\infty$ (100 mg, 0.305 mmol) was used instead of $[Au(C{\equiv}CPh)]_\infty$: yield 117 mg, 70%. ^{1}H NMR (270 MHz, CD_2Cl_2, 298 K, relative to TMS): δ 3.78 (s, 6H, −OMe), 6.75−7.34 (m, 8H, −C≡CPh), 7.48−7.64 (m, 24H, dppb). Positive FAB-MS: *m/z* 1103 $(M + 1)^+$, 971 $(M - C{\equiv}CPhOMe)^+$. IR (Nujol): ν/cm^{-1} 2116 (vw, C≡C). Anal. Calcd for $C_{48}H_{38}Au_2O_2P_2$: C, 52.27; H, 3.45. Found: C, 52.06; H, 3.23.

[Au_4(tppb)(C≡CC_6H_{13})$_4$] (4). To a benzene solution of $[Au(C{\equiv}CC_6H_{13})]_\infty$ (100 mg, 0.327 mmol) was added a solid sample of tppb (67 mg, 0.082 mmol). After it was stirred for 30 min in the dark, the solution was concentrated and yellow solid was precipitated by addition of *n*-hexane. Recrystallization was accomplished by the slow diffusion of *n*-hexane vapor into a benzene solution of the solid to give a yellow solid (yield 133 mg, 80%). The product should be kept in the absence of light. ^{1}H NMR (270 MHz, CD_2Cl_2, 298 K, relative to TMS): δ 0.89 (t, 12H, $-CH_3$), 1.12−1.51 (m, 32H, $-CH_2-$), 2.28 (m, 8H, $-C{\equiv}CCH_2-$), 7.12−7.50 (m, 42H, tppb). Positive FAB-MS: *m/z* 2037 $(M - 1)^+$, 1730 $(M - Au - \text{octynyl} - 2)^+$. IR (Nujol): ν/cm^{-1} 2130 (vw, C≡C). Anal. Calcd for $C_{86}H_{94}Au_4P_4$: C, 50.60; H, 4.61. Found: C, 50.30; H, 4.50.

[Au_4(tppb)(C≡CPh)$_4$] (5). To a yellow suspension of $[Au(C{\equiv}CPh)]_\infty$ (100 mg, 0.336 mmol) in CH_2Cl_2 was added a solid sample of tppb (68 mg, 0.084 mmol). A clear yellow solution was obtained, which was stirred for 30 min. The solution was then concentrated, and *n*-hexane was added to precipitate the yellow products. Recrystallization was accomplished by the slow diffusion of diethyl ether vapor into a dichloromethane solution of the solid to give yellow crystals (yield 118 mg, 70%). ^{1}H NMR (270 MHz, CD_2Cl_2, 298 K, relative to TMS): δ 7.06−7.57 (m, 20H, −C≡CPh; 42H, tppb). Positive FAB-MS: *m/z* 2006 $(M)^+$, 1905 $(M - C{\equiv}CPh)^+$. IR (Nujol): ν/cm^{-1} 2114 (vw, C≡C). Anal. Calcd for $C_{86}H_{62}Au_4P_4$: C, 51.45; H, 3.09. Found: C, 51.87; H, 2.98.

[Au_4(tppb)(C≡C(4-MeO-Ph))$_4$] (6). The procedures were similar to those for **5**, except $[Au(C{\equiv}C(4\text{-MeO-Ph})]_\infty$ (100 mg, 0.305 mmol) was used instead of $[Au(C{\equiv}CPh)]_\infty$: yield 135 mg, 83%. ^{1}H NMR (270 MHz, CD_2Cl_2, 298 K, relative to TMS): δ 3.79 (s, 12H, −OMe), 6.75−7.47 (m, 16H, −C≡CPh−; 42H, tppb). Positive FAB-MS: *m/z* 1995 $(M - C{\equiv}CPhOMe)^+$. IR (Nujol): ν/cm^{-1} 2101 (vw, C≡C). Anal. Calcd for $C_{90}H_{70}Au_4O_4P_4$: C, 50.80; H, 3.29. Found: C, 51.00; H, 3.05.

Physical Measurements and Instrumentation. UV−visible spectra were obtained on a Hewlett−Packard 8452A diode array spectrophotometer, IR spectra as Nujol mulls on a Bio-Rad FTS-7 Fourier-transform infrared spectrophotometer (4000−400 cm^{-1}), and steady-state excitation and emission spectra on a Spex Fluorolog 111 spectrofluorometer. Low-temperature (77 K) spectra were recorded by using an optical Dewar sample holder. ^{1}H NMR spectra were recorded on a JEOL JNM-GSX270 Fourier-transform NMR spectrometer with chemical shifts reported relative to TMS. Positive ion FAB mass spectra were recorded on a Finnigan MAT95 mass spectrometer. Elemental analyses of the new complexes were performed by Butterworth Laboratories Ltd.

Emission−lifetime measurements were performed using a conventional laser system. The excitation source was the 355-nm output (third harmonic) of a Quanta-Ray Q-switched GCR-150-10 pulsed Nd-YAG laser (10 Hz). Luminescence decay signals were recorded on a Tektronix Model TDS 620A digital oscilloscope and analyzed using a program for exponential fits. All solutions for photophysical studies were prepared under vacuum in a 10-cm^3 round-bottomed flask equipped with a side-arm 1-cm fluorescence cuvette and sealed from the atmosphere by a Kontes quick-release Teflon stopper. Solutions were rigorously degassed with no fewer than four freeze−pump−thaw cycles.

Crystal Structure Determination. Crystals of **2** and **5** were obtained by slow diffusion of diethyl ether vapor into a dichloromethane solution of the compounds. Diffraction data for **2** and **5** were measured at 25 °C on a Rigaku AFC7R diffractometer and a Nonius-Enraf CAD4 diffractometer, respectively, with graphite-monochromatized Mo Kα radiation (λ = 0.710 73 Å). Three standard reflections measured after every 300 reflections showed a decay of 16.64% for **2**, while for **5**, no decay was observed when three standard reflections were measured after every 2 h. The intensity data were corrected for Lorentz, polarization, and absorption effects. The empirical absorption corrections were based on azimuthal (ψ) scans of four strong reflections. Crystal and structure determination data for **2** and **5** are summarized in Table 1. The space group of **2** was uniquely determined from systematic absences, and that of **5** was confirmed by the successful refinement of the structure. Both structures were determined by heavy-atom Patterson methods and expanded using Fourier techniques[6] and refinement by full-matrix least squares using the MSC-Crystal Structure Package TEXSAN on a Silicon Graphics Indy computer. The complex molecules of both **2** and **5** consist of halves related by a center of symmetry at (0, 0, 1) and (0.5, 0.5, 0.5), respectively, at the center of the central ring system. All non-hydrogen atoms were refined anisotropically. Hydrogen atoms at calculated positions with thermal parameters equal to 1.3 times that of the attached carbon atoms were not refined. The final agreement factors for **2** and **5** are given in Table 1. The final atomic coordinates and thermal parameters of the non-hydrogen atoms of **2** and **5** are collected in Tables 2 and 3, respectively. The atomic coordinates of the hydrogen atoms of **2** and **5** are given in Tables SI and SII (Supporting Information), respectively.

Results and Discussion

Analogous to the preparation of monomeric gold alkynyl phosphine complexes of the type [RC≡CAu(PR$_3$)],[5a] reaction of $[Au(C{\equiv}CR)]_\infty$ with 0.5 equiv of the dppb ligand and 0.25 equiv of tppb in CH_2Cl_2 afforded the desired complexes [Au_2(dppb)(C≡CR)$_2$] and [Au_4(tppb)(C≡CR)$_4$], respectively, in greater than 70% yield. Subsequent recrystallization from a dichloromethane−diethyl ether mixture gave colorless to yellow crystals of **1**−**6**. Reaction of PhC≡CH with [Au_2(dppb)Cl$_2$] in the presence of KOH to give **2** has also been reported.[7h] All the newly synthesized compounds gave satisfactory elemental analyses and have been characterized by IR, positive FAB-MS, and ^{1}H NMR spectroscopy. Compounds **2** and **5** have also been characterized by X-ray crystallography.

The perspective drawings of **2** and **5** with atomic numberings are shown in Figures 1 and 2, respectively. Selected bond distances and angles are listed in Tables 4 and 5. In contrast to most Au(I) compounds, where

(6) PATTY & DIRDIF92: Beurskens, P. T.; Admiraal, G.; Beurskens, G.; Bosman, W. P.; Garcia-Granda, S.; Gould, R. O.; Smits, J. M. M.; Smykalla, C. The DIRDIF Program System; Technical Report of the Crystallography Laboratory; University of Nijmegen: Nijmegen, The Netherlands, 1992.

(7) (a) Yam, V. W.-W.; Lai, T. F.; Che, C. M. *J. Chem. Soc., Dalton Trans.* **1990**, 3747. (b) Stützer, A.; Bissinger, P.; Schmidbaur, H. *Chem. Ber.* **1992**, *125*, 367. (c) Dávila, R. M.; Stables, R. J.; Fackler, J. P., Jr. *Organometallics* **1994**, *13*, 418. (d) Angermaier, K.; Zeller, E.; Schmidbaur, H. *J. Organomet. Chem.* **1994**, *472*, 371. (e) Lin, I. J. B.; Hwang, J. M.; Feng, D. F.; Cheng, M. C.; Wang, Y. *Inorg. Chem.* **1994**, *33*, 3467. (f) Payne, N. C.; Ramachandran, R.; Puddephatt, R. J. *Can. J. Chem.* **1995**, *73*, 6. (g) Assefa, Z.; McBurnett, B. G.; Stables, R. J.; Fackler, J. P., Jr.; Assmann, B.; Angermaier, K.; Schmidbaur, H. *Inorg. Chem.* **1995**, *34*, 75. (h) Jia, G.; Puddephatt, R. J.; Scott, I. D.; Vittal, J. J. *Organometallics* **1993**, *12*, 3565.

Table 1. Crystal and Structure Determination Data for 2 and 5

	2	5
formula	$Au_2P_2C_{46}H_{34}$	$Au_4P_4C_{86}H_{62}$
fw	1042.66	2007.20
T, K	298	298
a, Å	9.217(5)	12.332(2)
b, Å	17.596(2)	12.520(3)
c, Å	11.842(4)	13.277(2)
α, deg	90	90.71(1)
β, deg	94.82(4)	90.59(1)
γ, deg	90	118.44(2)
V, Å^3	1913(1)	1802.1(6)
cryst syst	monoclinic	triclinic
space group	$P2_1/c$	$P\bar{1}$ (No. 2)
Z	2	1
F(000)	996	954
ρ_{calcd}, g cm^{-3}	1.809	1.849
cryst dimens, mm	0.15 × 0.10 × 0.25	0.10 × 0.07 × 0.25
λ, Å (graphite monochromated, Mo Kα)	0.710 73	0.710 73
μ(Mo Kα), cm^{-1}	77.99	82.78
transmissn factors	0.678−1.000	0.809−1.000
collecn range	$2\theta_{max}$ = 48° (h, 0−10; k, 0−20; l, −13 to +13)	$2\theta_{max}$ = 44° (h, 0−13; k, −13 to +13; l, −14 to +14)
scan mode; scan speed, deg min^{-1}	ω−2θ; 16.0	ω−2θ; 1.03−5.49
scan width, deg	1.21 + 0.35 tan θ	0.55 + 0.35 tan θ
no. of data collected	3337	4653
no. of unique data	3127	4400
R_{int}	0.023	0.015
no. of data used in refinement, m	1887 ($I > 3\sigma(I)$)	3405 ($I > 3\sigma(I)$)
no. of parameters refined, p	226	424
$R(F_o)$	0.028	0.021
$R_w(F_o)$	0.034[a]	0.021[b]
S	1.12	1.34
max shift, (shift/error)$_{max}$	0.01	0.01
residual extrema in final diff map, e Å^{-3}	+0.44, −0.61	+0.53, −0.36

[a] $w = 4F_o^2/\sigma^2(F_o^2)$, where $\sigma^2(F_o^2) = [\sigma^2(I) + (0.031F_o^2)^2]$. [b] $w = 4F_o^2/\sigma^2(F_o^2)$, where $\sigma^2(F_o^2) = [\sigma^2(I) + (0.005F_o^2)^2]$.

Table 2. Fractional Coordinates and Thermal Parameters[a] for Non-Hydrogen Atoms and Their Esd's for 2

atom	x	y	z	B_{eq}, Å^2
Au(1)	0.10254(4)	−0.07083(2)	0.65074(3)	4.382(9)
P(1)	−0.0231(3)	0.0241(1)	0.7289(2)	3.75(5)
C(1)	0.216(1)	−0.1578(6)	0.5941(8)	5.3(3)
C(2)	0.287(1)	−0.2094(5)	0.5676(8)	4.7(2)
C(3)	0.376(1)	−0.2702(5)	0.5311(9)	5.0(3)
C(4)	0.348(1)	−0.3043(5)	0.4259(9)	5.8(3)
C(5)	0.435(1)	−0.3623(6)	0.392(1)	6.7(3)
C(6)	0.546(2)	−0.3894(7)	0.460(1)	8.0(4)
C(7)	0.580(1)	−0.3557(8)	0.564(1)	8.5(4)
C(8)	0.493(1)	−0.2974(7)	0.5979(9)	7.1(3)
C(9)	−0.0128(9)	0.0117(5)	0.8822(7)	3.7(2)
C(10)	0.1111(10)	−0.0190(5)	0.9361(7)	4.5(2)
C(11)	0.1257(10)	−0.0312(5)	1.0518(8)	4.6(2)
C(12)	0.0460(8)	0.1189(5)	0.7045(7)	4.0(2)
C(13)	0.020(1)	0.1807(5)	0.7752(9)	6.0(3)
C(14)	0.073(1)	0.2510(6)	0.748(1)	7.8(4)
C(15)	0.150(1)	0.2612(6)	0.657(1)	8.1(4)
C(16)	0.179(1)	0.2030(7)	0.5888(10)	6.9(3)
C(17)	0.125(1)	0.1303(6)	0.6109(8)	5.1(3)
C(18)	−0.2166(9)	0.0230(5)	0.6872(7)	3.9(2)
C(19)	−0.301(1)	0.0880(5)	0.6795(8)	5.0(3)
C(20)	−0.452(1)	0.0832(7)	0.6531(10)	6.9(3)
C(21)	−0.513(1)	0.0130(8)	0.6397(9)	6.5(3)
C(22)	−0.430(1)	−0.0507(7)	0.6448(9)	6.5(3)
C(23)	−0.283(1)	−0.0467(5)	0.6687(8)	5.0(2)

[a] $B_{eq} = {}^8/_3\pi^2(U_{11}(aa^*)^2 + U_{22}(bb^*)^2 + U_{33}(cc^*)^2 + 2U_{12}aa^*bb^* \cos\gamma + 2U_{13}aa^*cc^* \cos\beta + 2U_{23}bb^*cc^* \cos\alpha)$.

there exist short Au···Au intermolecular contacts,[7a−g] no such short interactions are observed in **2** (Au···Au = 4.62 Å), as the bulky phenyl rings of the phosphine probably prevent their close approach. The torsion angle Au(1)−P(1)−C(9)−C(10), which defines the conformation of the alkynylgold unit with respect to the central phenyl ring, is 33.05°, and the dihedral angle between the phenyl planes of the phenylethynyl and the central phenyl unit is 37.83° in **2**. The Au−P bond distance of 2.273(2) Å in **2** is comparable to those observed in other alkynylgold phosphines[2c,7f,h] but longer than those of the chlorogold phosphine complexes,[7d,g] in line with the higher *trans* influence of the alkynyl group. The angles P(1)−Au(1)−C(1) of 175.5(3)° and Au(1)−C(1)−C(2) of 175.8(9)°, which are close to linearity and typical of sp hybridization in Au(I) and acetylenic carbon, are in the range found for other gold(I) phosphine and acetylide complexes.[2c,7f,h] Furthermore, the C≡C bond distance of 1.18(1) Å is typical of terminal acetylides. All other bond angles and bond lengths are normal.

Similarly, the bond lengths of Au−P (2.266(2) and 2.275(2) Å) and Au−C (1.996(7) and 1.998(7) Å) in **5** are normal. The bond angles of P−Au−C (174.3(2) and 174.2(2)°) and Au−C−C (175.6(7) and 171.9(6)°) are also near linearity. However, unlike **2**, short intramolecular Au···Au contacts of 3.1541(4) Å are found between adjacent Au units. Such distances are shorter than the sum of the van der Waals radii for Au and are comparable to Au···Au distances in other Au(I) phosphine complexes,[7] indicative of the presence of weak Au···Au interactions in the solid state. The dihedral angles between the phenyl planes of the phenylethynyl and the central phenyl unit are in the range 57.56−69.16°, with the two phenyl planes of the phenylethynyl units on the adjacent Au(1) and Au(2) at an angle of 12.76° to each other. The arrangement of the two adjacent Au(C≡CPh) groups is in a crossed geometry rather than a radial one, with a P(1)−Au(1)−Au(2)−P(2) torsion angle of 75.31(6)°. Consequently, the shape of the molecule is that of a distorted anthracene-like structure consist-

Table 3. Fractional Coordinates and Thermal Parameters[a] for Non-Hydrogen Atoms and Their Esd's for 5

atom	*x*	*y*	*z*	B_{eq}, Å^2
Au(1)	0.24500(2)	0.08004(2)	0.39822(2)	3.361(7)
Au(2)	0.28739(2)	0.25662(2)	0.21790(2)	3.331(7)
P(1)	0.2484(2)	0.2410(1)	0.4810(1)	2.96(4)
P(2)	0.4741(2)	0.3373(1)	0.2986(1)	2.76(4)
C(1)	0.2332(6)	−0.0717(6)	0.3371(5)	3.8(2)
C(2)	0.2347(7)	−0.1576(7)	0.3007(5)	4.5(2)
C(3)	0.2389(8)	−0.2611(7)	0.2549(6)	4.9(2)
C(4)	0.1540(8)	−0.3355(8)	0.1873(8)	7.3(3)
C(5)	0.158(1)	−0.4345(9)	0.1434(8)	9.0(4)
C(6)	0.249(1)	−0.4584(10)	0.1722(9)	9.6(4)
C(7)	0.340(1)	−0.383(1)	0.2397(9)	10.1(4)
C(8)	0.332(1)	−0.2884(9)	0.2796(7)	8.0(3)
C(9)	0.1296(7)	0.2021(6)	0.1402(5)	3.8(2)
C(10)	0.0337(7)	0.1799(6)	0.1007(5)	3.9(2)
C(11)	−0.0844(6)	0.1534(6)	0.0556(5)	3.8(2)
C(12)	−0.1458(8)	0.2122(8)	0.0881(6)	6.1(3)
C(13)	−0.2614(10)	0.184(1)	0.0450(8)	7.7(3)
C(14)	−0.3161(9)	0.092(1)	−0.0244(8)	8.3(3)
C(15)	−0.2533(9)	0.0334(9)	−0.0575(7)	6.9(3)
C(16)	−0.1396(7)	0.0632(7)	−0.0171(5)	4.8(2)
C(17)	0.1347(6)	0.2821(6)	0.4346(5)	3.3(2)
C(18)	0.1474(8)	0.3977(7)	0.4439(7)	5.8(2)
C(19)	0.0554(10)	0.4222(9)	0.4095(8)	8.0(3)
C(20)	−0.0494(9)	0.331(1)	0.3680(8)	7.7(3)
C(21)	−0.0637(8)	0.216(1)	0.3604(7)	7.3(3)
C(22)	0.0276(7)	0.1917(7)	0.3916(6)	5.1(2)
C(23)	0.2119(6)	0.2011(5)	0.6118(5)	3.0(2)
C(24)	0.2923(7)	0.1797(7)	0.6701(6)	4.9(2)
C(25)	0.2629(9)	0.1392(8)	0.7681(6)	5.8(3)
C(26)	0.1521(10)	0.1213(7)	0.8051(6)	6.1(3)
C(27)	0.0710(7)	0.1422(7)	0.7498(6)	5.6(2)
C(28)	0.1002(7)	0.1815(6)	0.6523(5)	4.5(2)
C(29)	0.5281(6)	0.2321(5)	0.3377(5)	2.8(2)
C(30)	0.5230(7)	0.1480(7)	0.2680(5)	4.4(2)
C(31)	0.5660(8)	0.0681(7)	0.2913(7)	5.7(2)
C(32)	0.6127(7)	0.0721(7)	0.3840(8)	5.7(3)
C(33)	0.6191(8)	0.1542(8)	0.4550(6)	6.0(3)
C(34)	0.5774(7)	0.2363(6)	0.4319(5)	4.3(2)
C(35)	0.5961(6)	0.4406(6)	0.2181(5)	3.3(2)
C(36)	0.5714(7)	0.5040(7)	0.1456(5)	4.9(2)
C(37)	0.664(1)	0.5813(8)	0.0825(6)	6.9(3)
C(38)	0.778(1)	0.5915(9)	0.0918(8)	7.6(3)
C(39)	0.8048(9)	0.5291(9)	0.1620(9)	7.7(3)
C(40)	0.7144(8)	0.4538(7)	0.2251(6)	5.3(2)
C(41)	0.3946(5)	0.3860(5)	0.4884(4)	2.4(1)
C(42)	0.4843(5)	0.4264(5)	0.4142(4)	2.3(1)
C(43)	0.5872(6)	0.5398(5)	0.4277(4)	2.7(2)

[a] See footnote *a* in Table 2.

ing of a central benzene ring with two fused Au_2PC_2P six-membered rings at the two opposite sides, as compared to the three fused benzene rings in anthracene. This arises as a result of the presence of weak Au···Au interactions, which hold the two Au(C≡CPh) units together, although such a structure may also be favored on steric grounds. In order to minimize the steric repulsion between the phenyl rings on the neighboring PPh_2 groups, the rings may prefer to get rid of each other by the rotation of the P−C σ bonds such that the two Au atoms are forced to approach each other. However, given the ability of the acetylenic moieties of a related *cis*-$PtMe_2(Ph_2PC{\equiv}CPh)_2$ system to adopt a noncrossed geometry,[8] it is believed that auriophilicity plays a crucial role in dictating the structure of **5**.

The electronic absorption spectra of the complexes **1**−**6** and the related Au(PPh_3)(C≡CPh) (**7**)[2c] in dichloromethane at room temperature show intense absorption bands at *ca*. 250−300 nm. With reference to previous work on ethynylgold(I) complexes[2c] and the similarities of the absorption bands with the corresponding ligands, the bands are assigned as the $\sigma \rightarrow \pi^*$ (Ph_{bridge}) transition. This type of transition involves the promotion of an electron from the phosphorus lone-pair orbital σ-bonded to an Au atom to the empty antibonding orbital of π origin situated on the bridging phenyl group of the phosphine. From the absorption spectra of the ligands dppb and tppb, as compared to PPh_3, it is shown that the transition energy of their lowest lying

(8) Johnson, D. K.; Rukachaisirikul, T.; Sun, Y.; Taylor, N. J.; Canty, A. J.; Carty, A. J. *Inorg. Chem.* **1993**, *32*, 5544.

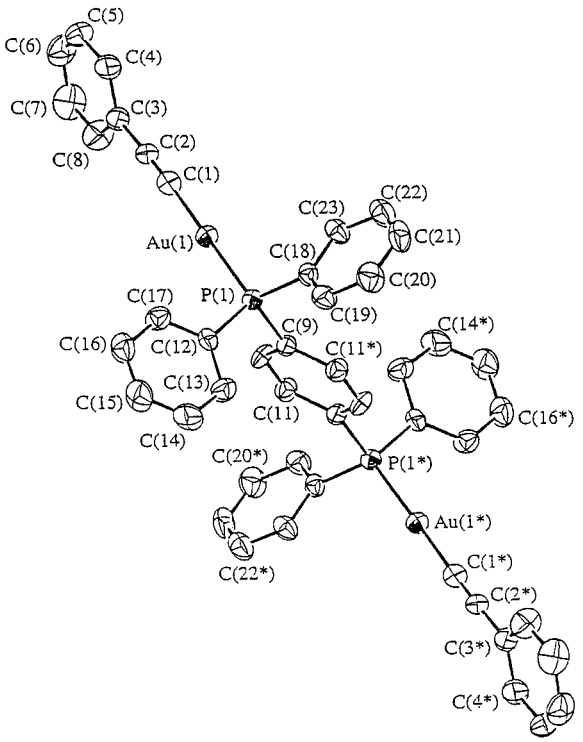

Figure 1. Perspective drawing of complex of **2** with the atomic numbering scheme. Thermal ellipsoids are shown at the 30% probability level. The starred atoms have fractional coordinates at (−*x*, −*y*, 2 − *z*).

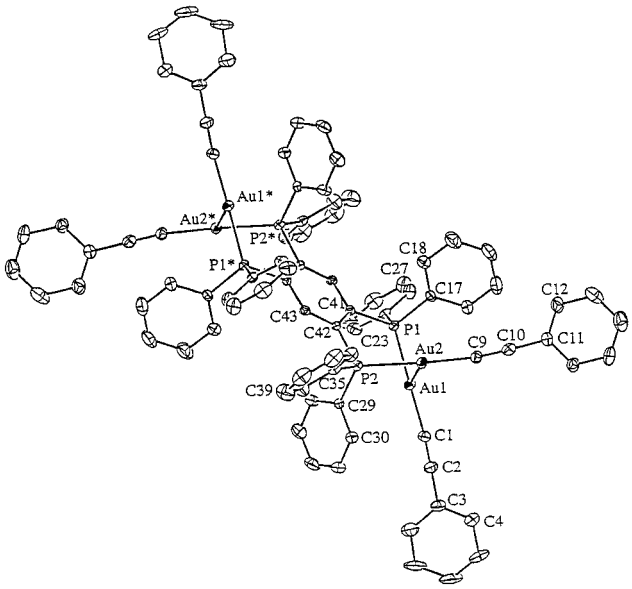

Figure 2. Perspective drawing of the complex of **5** with atomic numbering scheme. Thermal ellipsoids are shown at the 25% probability level. The starred atoms have fractional coordinates at (1 − *x*, 1 − *y*, 1 − *z*).

Table 4. Selected Bond Lengths (Å) and Angles (deg) with Estimated Standard Deviations (Esd's) in Parentheses for 2

Bond Lengths			
Au(1)−P(1)	2.273(2)	C(1)−C(2)	1.18(1)
Au(1)−C(1)	2.00(1)		
Bond Angles			
P(1)−Au(1)−C(1)	175.5(3)	C(9)−P(1)−C(18)	103.8(4)
Au(1)−P(1)−C(9)	109.4(3)	C(12)−P(1)−C(18)	108.4(4)
Au(1)−P(1)−C(12)	114.3(3)	Au(1)−C(1)−C(2)	175.8(9)
Au(1)−P(1)−C(18)	113.9(3)	C(1)−C(2)−C(3)	177.0(1)
C(9)−P(1)−C(12)	106.2(4)		

Table 5. Selected Bond Lengths (Å) and Angles (deg) with Estimated Standard Deviations (Esd's) in Parentheses for 5

Bond Lengths			
Au(1)−Au(2)	3.1541(4)	Au(2)−C(9)	1.998(7)
Au(1)−P(1)	2.266(2)	C(1)−C(2)	1.182(9)
Au(1)−C(1)	1.996(7)	C(9)−C(10)	1.193(9)
Au(2)−P(2)	2.275(2)		
Bond Angles			
Au(2)−Au(1)−P(1)	79.31(4)	Au(1)−P(1)−C(23)	108.3(2)
Au(2)−Au(1)−C(1)	106.0(2)	Au(1)−P(1)−C(41)	118.9(2)
P(1)−Au(1)−C(1)	174.3(2)	Au(2)−P(2)−C(29)	117.0(2)
P(2)−Au(2)−C(9)	174.2(2)	Au(2)−P(2)−C(35)	111.1(2)
Au(1)−Au(2)−P(2)	75.86(4)	Au(1)−C(1)−C(2)	175.6(7)
Au(1)−Au(2)−C(9)	109.7(2)	C(1)−C(2)−C(3)	178.7(8)
P(2)−Au(2)−C(9)	174.2(2)	Au(2)−C(9)−C(10)	171.9(6)
Au(1)−P(1)−C(17)	113.9(2)	C(9)−C(10)−C(11)	178.3(8)

absorption bands is in the order $PPh_3 \approx$ dppb > tppb. This is understandable, since increasing the number of PPh_2 groups attached to the central phenyl ring would render the ring more electron deficient, thus lowering the corresponding π^* level, which results in a red shift in transition energy. A comparison of the electronic absorption data with those for **7** shows that the absorption energy of **7** is similar to that for **2** but greater than that for **5**, similar to the trend observed for the corresponding phosphines. It is also interesting to note that the extinction coefficients of the low-energy absorption bands of **5** are roughly twice that of **2** and four times that of **7**, which roughly parallel the number of Au(PhC≡C) units in the complexes, confirming their assignment as $\sigma \rightarrow \pi^*$ (Ph_{bridge}) transitions. Such enhancements in the absorption coefficients when the number of chromophoric units is increased may find useful applications in the design of light harvesting devices.

Excitation of the complexes at λ > 350 nm both in the solid state and in dichloromethane solution results in long-lived intense luminescence. Figure 3 shows the solid-state excitation and emission spectra of **5**, and the photophysical data for **1**−**7** are summarized in Table 6. The solid-state emission spectra of dppb, **1**, and **2** are very similar in energy, with an intense emission centered at *ca*. 500 nm, which is at higher energy than that of **3**. The long lifetime of the emission in the microsecond range suggests that it is most likely associated with a spin-forbidden transition. The emission of **3** is red-shifted relative to **2**. This can be rationalized by the fact that the −OMe group on the acetylide is electron-donating in nature, which reduces the extent of metal to ligand back-π-donation (d_π(Au) → π^*(−C≡CR)) to the acetylide, leading to an increased d_π(Au)−3d(P) overlap and hence resulting in a reinforced Au−P bond via the synergistic effect. The same is observed for **5** and **6** (611 nm for **5** *vs* 628 nm for **6**). Similarly,

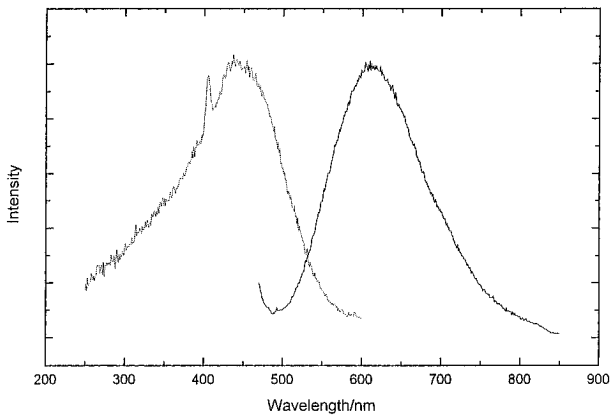

Figure 3. Solid-state emission (solid line) and excitation (dotted line) spectra of ground **5** at 25 °C.

Table 6. Electronic Absorption and Emission Data for Compounds 1−7

		emissn[b]	
compd	abs[a] λ_{max}/nm (ϵ/dm^3 mol^{-1} cm^{-1})	medium (T/K)	λ_{max}/nm (τ_0/μs)
1	256 (38 400)	solid (298)	510 (153.8)
	268 (sh) (26 870)	solid (77)	427, 537
	275 (sh) (18 735)	CH_2Cl_2 (298)	392 (0.67)
	284 (sh) (6 070)		587[d] (0.93)
2	259 (53 440)	solid (298)	507 (5.32)
	270 (63 470)	solid (298)[c]	505 (sh) (1.20), 590, 631[d] (4.44)
	283 (57 060)	solid (77)	483
		solid (77)[c]	507, 596, 617[d]
		CH_2Cl_2 (298)	395, 411 (sh), 476 (sh), 601 (sh)
			628[d] (0.27)
3	261 (48 070)	solid (298)	486, 563[e] (5.06)
	270 (50 335)	solid (77)	483, 556[e]
	275 (49 710)	CH_2Cl_2 (298)	395, 462 (sh), 541 (2.66)
	285 (47 880)		
	299 (40 590)		
4	289 (sh) (37 715)	solid (298)	405, 602 (1.28)
	355 (sh) (5 620)	solid (77)	586
		CH_2Cl_2 (298)	409, 577 (0.71)
5	241 (sh) (138 455)	solid (298)	599, 611[e] (0.57)
	271 (sh) (102 320)	solid (298)[c]	529 (2.52)
	365 (sh) (9 400)	solid (77)	584, 611[e]
		solid (77)[c]	529, 569[e]
		CH_2Cl_2 (298)	510, 538 (sh) (0.46)
6	262 (sh) (133 850)	solid (298)	415, 628[e] (1.85)
	276 (133 895)	solid (77)	414, 618[e]
	288 (sh) (126 185)	CH_2Cl_2 (298)	447, 601 (0.47)
	302 (sh) (103 260)		
	370 (sh) (10 945)		
7[f]	238 (32 000)	solid (298)	459 (33.4)
	271 (19 400)	solid (77)	457
	291 (sh) (11 400)	CH_2Cl_2 (298)	410, 454 (sh) (6.6)
dppb	274 (18 640)	solid (298)	409, 500 (sh)
		solid (77)	443
		CH_2Cl_2 (298)	402, 510, 546 (sh)
tppb	245 (sh) (27 720)	solid (298)	466, 495
	261 (22 770)	solid (77)	502, 547
	329 (sh) (4 965)	CH_2Cl_2 (298)	509, 544 (sh)

[a] All absorption spectra are recorded using CH_2Cl_2 as solvent at 298 K. [b] Excitation wavelength is 350 nm. [c] Crystalline unground samples were used for measurement. [d] Excitation wavelength is 500 nm. [e] Excitation wavelength is 450 nm. [f] From ref 2c.

the solution luminescence of **1** and **2** shows very similar emission energy maxima and patterns with a high-energy band at *ca*. 395 nm and a low-energy emission

at *ca.* 600 nm. The former is likely to be $\pi \rightarrow \pi^*$ (Ph_{bridge}) and the latter is likely to be $\sigma \rightarrow \pi^*$ (Ph_{bridge}) in origin. An alternative assignment of the lowest lying excited state as metal-to-ligand charge transfer (MLCT, d(Au) $\rightarrow \pi^*$(C≡CR)) in **1**−**3** and metal−metal-bond-to-ligand charge transfer (MMLCT, d_{σ^*}(Au) or d_{δ^*}(Au) $\rightarrow \pi^*$(C≡CR)) in **4**−**6**, which also gives rise to an observed red shift in emission energy on going from **1**−**3** to **4**−**6** (Au···Au for **5**, 3.1541(4) Å), has been precluded, owing to the fact that the emission energies did not comply with the π^*(C≡CR) energy level of the acetylides, where an order of orbital energies of $\pi^*(C{\equiv}CC_6H_{13}) > \pi^*(C{\equiv}CPhOMe) > \pi^*(C{\equiv}CPh)$ is expected. An assignment of the origin of emission for **1**−**3** in the solid state from a MMLCT is also unlikely, owing to the large intermolecular Au···Au separation (**2**, 4.62 Å).

Furthermore, it is interesting to note that the solid-state emissions of **2** and **5**, both at room temperature and 77 K, show different emission maxima for the crystalline unground and fully ground samples. Emission energy decreases for a ground sample of **2** as compared to a crystalline unground sample, while the reverse is observed for ground and crystalline unground samples of **5**. It is likely that the degree of solvent incorporation in the crystalline samples of **2** and **5** plays an important role in governing the energy of the emissive states.

It should be mentioned that, unlike Au(I) phosphine complexes such as $[Au_3(dmmp)_2]^{3+}$,[7a] the origin of the luminescence for complexes **1**−**6** is consistent with a $\sigma \rightarrow \pi^*$ (Ph_{bridge}) excited state and the presence of an Au···Au interaction in **5** would not be expected to perturb the origin of the luminescent state.

Preparations of analogous complexes with longer aliphatic acetylene derivatives and investigations of their liquid crystalline properties are in progress.

Acknowledgment. V.W.-W.Y. acknowledges financial support from the Research Grants Council, the Croucher Foundation, and The University of Hong Kong. S.W.-K.C. acknowledges the receipt of a postgraduate studentship and a Swire Scholarship, administered by The University of Hong Kong.

Supporting Information Available: Text giving details of the crystal structure solutions and tables giving fractional coordinates and thermal parameters for hydrogen atoms, general displacement parameter expressions *U*, and all bond distances and bond angles for **2** and **5** (20 pages). Ordering information is given on any current masthead page.

OM950586B